microPublication BIOLOGY

11/11/2026 - *Open Access*

An Arabidopsis *RALF17 (AT2G32885)* GABI-Kat T-DNA line with two insertions has reproductive defects in the hemizygous state, possibly due to a genomic rearrangement

Jen Sloan[1], Yui-Leung Lau[2], Amber Gentle[2], Ellen Allwood[1], Volkan Cevik[2], James Doughty[2], Lisa M Smith[1§]

[1]School of Biosciences, University of Sheffield

[2]Department of Life Sciences, University of Bath

[§]To whom correspondence should be addressed: Lisa.m.smith@sheffield.ac.uk

Abstract

T-DNA insertion lines are reported to have a high probability of chromosomal rearrangements such as translocations, which can result in gametophytic developmental defects. Here we report pollen and ovule phenotypes in a *RALF17 (AT2G32885)* GABI-Kat line that are present only when the T-DNA is in a hemizygous state, including misshapen mature pollen and an accumulation of callose in the embryo sac. These observations are consistent with phenotypes resulting from chromosomal translocations, often associated with multiple T-DNAs, and we confirmed presence of a second T-DNA insertion. We urge the research community to use alternative knockout lines for reproductive studies of *RALF17*.

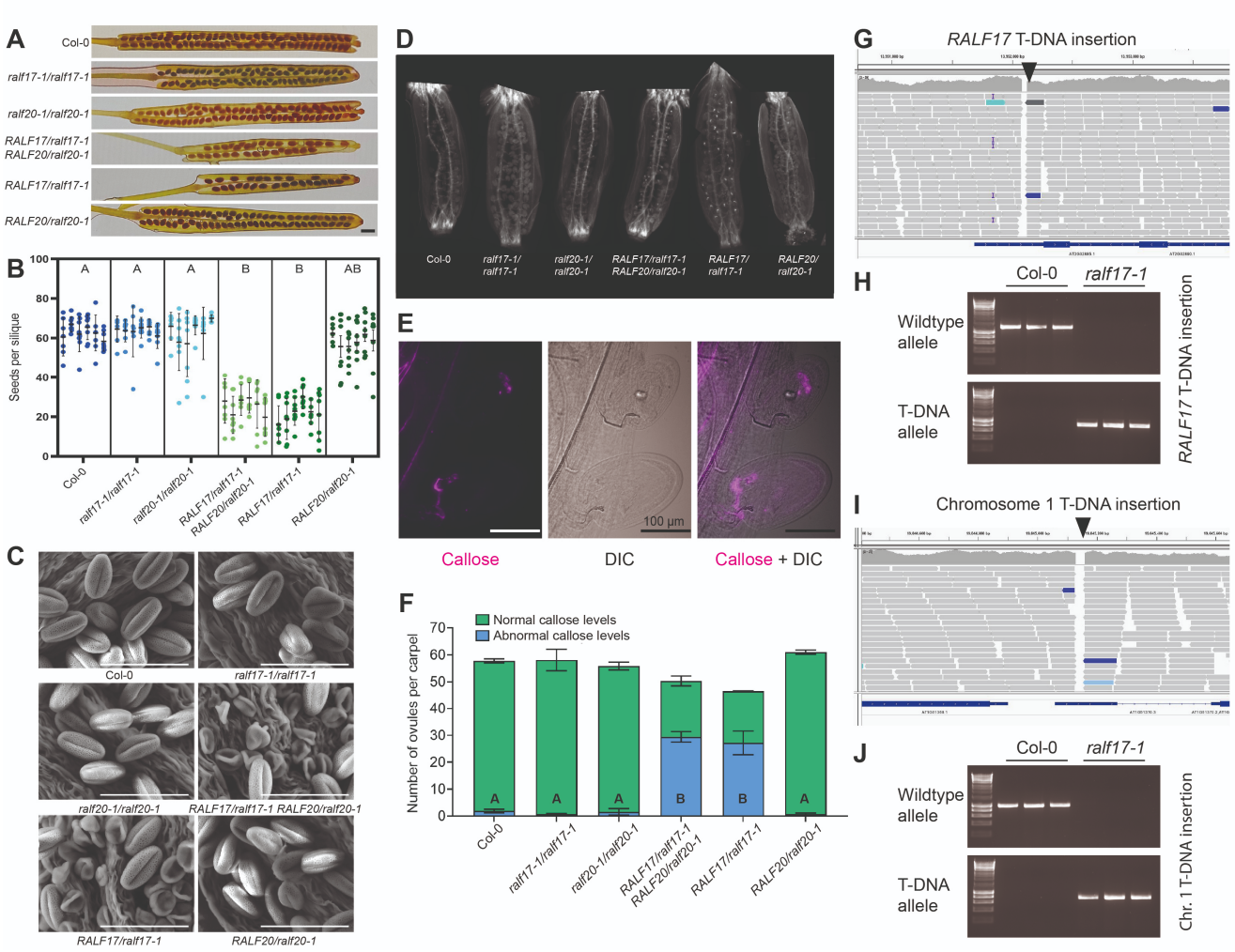


Figure 1. The *RALF17* GABI-Kat T-DNA insertion line has gametophytic defects when in a hemizygous state:

A: Cleared siliques of genotypes used in this study showing a reduced number of seeds in lines where the *ralf17-1* GABI-Kat T-DNA insertion of stock line GK_699G03.03 is hemizygous but not homozygous. Scale bar 1 mm. **B:** Seeds counts for each genotype (6 plants per genotype, 7-8 siliques per plant) show lower numbers of seeds are produced when *ralf17-1* is hemizygous in either a cross to wildtype Col-0 or the *ralf20-1* T-DNA insertion. Letters refer to statistically similar

groups based Kruskal-Wallis test with a post hoc Dunn's multiple comparisons test. **C:** SEM images of pollen grains on mature anthers for each genotype showing pollen defects in the F1 progeny of *ralf17-1/ralf17-1* x Col-0 and *ralf17-1/ralf17-1* x *ralf20-1/ralf20-1* crosses. Scale bar 100 µm. **D:** Composite image of aniline blue (sirofluor)-stained carpels of each genotype. Callose deposits can be observed in approximately half of the ovules in carpels from F1 progeny of *ralf17-1/ralf17-1* x Col-0 and *ralf17-1/ralf17-1* x *ralf20-1/ralf20-1* crosses. Anthers were removed prior to dehiscence and carpels stained 48 hours after anther removal to ensure ovule maturity. **E**: Epifluorescence image of callose staining of two ovules from a *RALF17/ralf17-1 RALF20/ralf20-1* plant showing abnormal callose deposition in the embryo sac of the upper ovule compared to a normal ovule below. **F:** Quantification of the number of ovules with abnormal vs normal callose levels in the embryo sac for each genotype used in this study. Ovules from 2-3 siliques per plant for 3 plants per line were categorised according to callose level. Means from each plant were used to calculate standard error of the mean. Significantly more ovules had abnormal levels of callose in the *RALF17/ralf17-1 RALF20/ralf20-1 and RALF17/ralf17-1* plant compared to Col-0, with letters referring to statistically similar groups based on pair-wise Chi-squared tests with correction for multiple testing. **G**: Mapping of Illumina reads against the *ralf17-1* gene model confirms insertion in the 5' UTR. The upper grey histogram indicates read depth, with grey lines below showing individual reads. The gene model is shown below in blue, while a black arrow indicates the insertion site. **H:** PCR genotyping confirmed the GABI-Kat T-DNA insertion in *RALF17* for three *ralf17-1* plants, while only the wildtype allele is detected for three Col-0 plants. **I**: Mapping of Illumina reads indicates a second GABI-Kat insertion in the 5' UTR of *AT1G51370*. As per G, the upper grey histogram indicates read depth, with grey lines below showing individual reads. The gene model is shown below in blue, while a black arrow indicates the insertion site. **J:** PCR genotyping confirmed presence of the GABI-Kat T-DNA backbone in *AT1G51370* for three *ralf17-1* plants.

Description

While studying the effects of RALF peptides on reproduction in Arabidopsis, we noted reduced seed set in F1 lines containing a *RALF17* (*At2G32885;* as per (Abarca *et al*., 2021)) GABI-Kat T-DNA insertion (GK_699G03.03, N467083) in the hemizygous state, but no effect on seed set in homozygous lines. Given reports of genomic rearrangements causing similar phenotypes (Alling and Galindo-Trigo, 2023), we describe here our phenotypic observations and genotyping in order to alert the Arabidopsis research community to issues with this specific plant line.

A *ralf17-1 ralf20-1* cross was performed due to potential functions of the cognate proteins in pollen grain hydration and an unexpected reduction in seed number per silique was noted in the F1 generation (i.e. plants hemizygous for both T-DNA insertions) (Lau, 2023). Production of a homozygous double mutant was not possible due to the linkage of the two genes (*AT2G32885* and *AT2G34825*). However, normal seed set was observed for each individual T-DNA insertion line in a homozygous state, indicating the observed phenotype was not due to lethality of one or other of the gene knockouts during gamete development.

To assess the extent of the seed development phenotype in the *RALF17/ralf17-1 RALF20/ralf20-1* F1 plants, siliques were cleared and seeds counted in comparison to the homozygous single T-DNA lines and a Col-0 wildtype control. The F1 plants had significantly fewer seeds than the Col-0, *ralf17-1/ralf17-1* or *ralf20-1/ralf20-1* controls (**Fig. 1A,B**; Kruskal-Wallis test; Col-0 vs F1 $p = 0.01$, *ralf17-1* vs F1 $p = 0.002$, *ralf20-1* vs F1 $p = 0.01$), with a mean of 25.6 seeds per F1 silique compared to 62.7 in Col-0, 64.0 in *ralf17-1* and 63.4 in *ralf20-1*. While the F1 plants produce fewer than half as many seeds, it was unclear which aspect of reproduction was affected (e.g. gamete development, pollen tube growth, pollen tube reception or seed development), and whether the *RALF17* or *RALF20* T-DNA insertion was the genetic determinant.

To determine which of the *RALF17* or *RALF20* T-DNA insertions was responsible for the observed reduction in seed set, the *ralf17-1* and *ralf20-1* homozygous lines were each backcrossed to Col-0 and seed numbers in the F1 generation counted. With seed counts in the *RALF17/ralf17-1* plants averaging 22.0 compared to a mean of 58.8 in the *RALF20/ralf20-1* plants (**Fig. 1A,B**), the *RALF17* T-DNA insertion was determined to be causal.

Crosses with the wildtype Col-0 line further explored the genetics of the phenotype. As the two T-DNAs are linked, non-Mendelian inheritance in a 1:1 ratio is expected in the seeds of a cross to Col-0. Genotyping of 99 seedlings from the Col-0 (female) x *RALF17/ralf17-1 RALF20/ralf20-1* (male) cross demonstrated equal transmission of the two T-DNAs via pollen (47 and 52 progeny hemizygous for the *ralf17-1* and *ralf20-1* T-DNAs, respectively; Chi-squared test $p = 0.62$). In contrast, transmission of the two T-DNA insertions via the female lineage in a *RALF17/ralf17-1 RALF20/ralf20-1* x Col-0 cross indicated reduced inheritance of the *ralf17-1* T-DNA (35 and 56 progeny inheriting the *ralf17-1* and *ralf20-1* T-DNAs, respectively; Chi-squared test $p = 0.03$). Thus, viable pollen grain formation is not significantly affected in the F1 *RALF17/ralf17-1 RALF20/ralf20-1* plants, while *ralf17-1* haploid ovules may have reduced viability.

To further understand the *ralf17-1* hemizygous phenotype, we examined gamete development, including pollen grains despite the lack of transmission effect. Pollen structure was examined through imaging with a scanning electron microscope. The wildtype Col-0 line and both single mutants had elongated pollen grains with three evenly spaced apertures and a regular exine pattern. A high proportion of the pollen grains of the *RALF17/ralf17-1 RALF20/ralf20-1*

plants were much smaller and more rounded with wider, less regular apertures and an irregular, less defined exine pattern (**Fig. 1C**). The F1 *RALF17/ralf17-1* had pollen grains similar to the double mutant, with many pollen grains having the smaller, irregular shape. *RALF20/ralf20-1* pollen grains, however, were comparable to Col-0 or the single homozygous mutants. Therefore, although transmission of the T-DNA insertions via pollen appears unaffected by whether the haploid genome contains the *ralf17-1* or *ralf20-1* T-DNA insertion, pollen grain development is nonetheless affected by hemizygousity of the *ralf17-1* T-DNA insertion in the parental plant.

Female gamete development was examined through callose staining of unfertilised carpels (48 hrs after emasculation to ensure mature ovules). Unfertilised, mature ovules in the *RALF17/ralf17-1 RALF20/ralf20-1* plants could be separated into two categories - those with limited/no callose deposition in the embryo sac that are comparable to ovules of wildtype Col-0 and those with increased deposition of callose in the embryo sac (**Fig. 1D,E**). These two categories of embryo sacs were observed at 45% (normal) and 55% (increased callose) frequency in *RALF17/ralf17-1 RALF20/ralf20-1* plants (**Fig. 1F**). Examining earlier stages of ovule development in Col-0, we did not observe callose deposition in the embryo sacs, indicating that this is ectopic callose deposition rather than a delay or cessation of ovule development. Combined with the T-DNA insertion transmission rates and seed set numbers presented above, the embryo sac phenotype does not appear to strictly correlate with a lack of viability of the ovules, as otherwise we would expect a much stronger effect on T-DNA insertion transmission via the female lineage and an inability to obtain homozygous *ralf17-1* plants. Aberrant embryo sac development could alternatively be a function of genomic rearrangements which lead to developmental defects rather than arising from hemizygousity of the *ralf17-1* T-DNA insertion per se.

Whole genome Illumina sequencing was undertaken to identify if a second T-DNA insertion is present in the *ralf17-1* GABI-Kat line. As well as confirming the T-DNA insertion in *RALF17* (**Fig. 1G,H**), a second insertion on chromosome 1 at *AT1G51370* (encoding an uncharacterised F-box protein) was identified based on a gap in reads mapped to the *Arabidopsis thaliana* genome (**Fig. 1I**) and mapping of read contigs to the pGABI1 plasmid. This insertion, confirmed by PCR (**Fig. 1J**), consists of the plasmid backbone between the right and left T-DNA borders of the pGABI1 plasmid, explaining why it was not identified during standard T-DNA line characterisation. Our mapping approach cannot address whether there is a genomic rearrangement incorporating these two T-DNA insertions as individual reads do not span the insertions.

The ovules and pollen grain phenotypes we have observed in plants hemizygous for the *ralf17-1* T-DNA insertion are consistent with phenotypes previously reported for other T-DNA insertion lines with genomic rearrangements. Reports of chromosomal translocations in non-T-DNA-containing plant lines of Datura and maize, that result in meiotic and gametophytic defects, date back a century (Belling and Blakeslee, 1926). With the advent of T-DNA lines for genetics research, genomic rearrangements became a more frequent pitfall. A number of studies have reported gametophytic defects and chromosomal translocations in individual Arabidopsis T-DNA lines (e.g. (Curtis *et al.*, 2009, Alling and Galindo-Trigo, 2023)). One study of 64 SALK T-DNA lines found a 19% rate of chromosomal translocations (Clark and Krysan, 2010) indicating the prevalence of this issue. A smaller study which sequenced the genomes of 14 GABI-Kat T-DNA insertion lines identified chromosomal translocations in four lines, along with numerous T-DNA insertion sites that had not been annotated, concluding that GABI-Kat lines may contain an average of two T-DNA insertions (Pucker *et al.*, 2021). The presence of multiple T-DNA insertions is not however required for chromosomal translocations to occur in insertion lines (reviewed in (Thomson *et al.*, 2024)). As recently highlighted by (Raabe *et al.*, 2024), the gametophytic effects of potential chromosomal rearrangements are of particular concern when studying plant reproduction, with screening of gametophyte phenotypes in F1 crosses of particular relevance. Here we would add our voice to those of others, urging caution when gametophytic phenotypes are observed in hemizygous T-DNA insertion lines but not cognate homozygous lines, with particular warning regarding the RALF17 GABI-Kat T-DNA insertion line GK_699G03.03, NASC N467083.

Methods

Plant growth

The *ralf17-1* and *ralf20-1* T-DNA insertion lines (GK_699G03.03 and SALK_089411C, respectively; (Alonso *et al.*, 2003, Kleinboelting *et al.*, 2012)) were acquired from the Nottingham Arabidopsis Stock Centre. Plants were grown in a 3:1 mix of Levington M3 compost:sand in a Conviron growth chamber. Set growth conditions were 22ºC, ~150 µmol^{-1}m^{-2} light from LEDs for 16 hrs per day and 60% humidity. Genotyping used Qiagen multiplex PCR mix (catalogue number 206143) as per the manufacturer's guidance, with primers as per the sequences below.

Developmental imaging

For seed counts, mature siliques (7-8 per plant from 6 plants per genotype) were cleared for 2-4 days in 0.4 M NaOH 1% Triton-X 100 at room temperature before photographs were taken. Seed counts were scored from the photographs.

For pollen imaging, anthers were mounted onto aluminium stubs with carbon tabs (Agar Scientific) and imaged using a Hitachi TM3030Plus benchtop scanning electron microscope in secondary electron mode at 15kV.

For aniline blue/sirofluor staining of ovules (Conrath, 2024), anthers were removed from the flowers (stage 16) prior to dehiscence and unpollinated carpels collected 48 hrs later to ensure ovule maturity. Staining and imaging with a Leica DM6 epifluorescence microscope were as described in (Galindo-Trigo *et al.*, 2020). Ovule phenotypes were categorised for 2-3 carpels per plant and 3 plants per genotype.

Statistics

Seed counts were compared using a Kruskal-Wallis test with correction for multiple testing (Dunn's multiple comparisons test) performed in GraphPad Prism v 10.0.2. T-DNA insertion transmission rates were analysed in Microsoft Excel (v 16.90.02) using a Chi-square test.

T-DNA insertion mapping

To identify T-DNA insertion sites in the *ralf17-1* mutant, genomic DNA was extracted from 3-week-old plants using the DNeasy Plant Maxi Kit (Qiagen). The DNA sample was submitted to Novagene for Illumina sequencing to generate 150-bp paired-end reads. The raw sequencing reads were processed using Fastp (Chen *et al.*, 2018) to remove adapter sequences and trim low-quality bases. The resulting filtered reads were initially mapped to the *Arabidopsis thaliana* reference genome (TAIR10) using the Burrows-Wheeler Aligner (BWA; (Li and Durbin, 2010)). The resulting SAM files were converted to sorted BAM files using SAMtools (Li *et al.*, 2009). The sorted BAM files were then visualised using Integrative Genomics Viewer (IGV), version 2.19.8 (Robinson *et al.*, 2011), allowing the T-DNA integration site in *ralf17-1* to be identified.

To determine whether additional T-DNA integrations were present in the mutant, the filtered Illumina sequencing reads were used to generate *de novo* genome assemblies for *ralf17-1* using SPAdes Genome Assembler, version 4.3.0 (Prjibelski *et al.*, 2020). The *ralf17-1* assembly consisted of 4,728 contigs, with a total assembly length of 124,456,250 bp and an N50 of 100,402 bp.

The genome assembly was subsequently searched for sequences derived from the full-length pGABI1 plasmid sequence using BLAST+ (Camacho *et al.*, 2009). BLAST hits corresponding to plasmid-derived sequences were then examined to identify contigs containing T-DNA sequences and to assess the possibility of additional T-DNA integration sites.

Reagents

Genotype	**Gene**	**ID**	**Source**
Col-0	-	-	
Col-0 *ralf17-1*	*At2g32885*	GK_699G03.03	NASC N467083
Col-0 *ralf20-1*	*At2g34825*	SALK_089411C	NASC N671676

Primer name	**Primer sequence**
SALK T-DNA (for RALF20 genotyping)	ATTTTGCCGATTTCGGAAC
GK T-DNA (for RALF17 genotyping)	CATTTTATAATAACGCTGCGGACATCTAC
RALF17fw	AATGCTACCACATGAACTGGC
RALF17rv	GTACCAGTCTCAGCTTGCTGC
RALF20fw	TATCCTCTCACGATGGGACAC
RALF20rv	TGATCATTTCTTTCACTGGCAG
At1g51360fw	TGGAAGAAGCGAAATTGGAGA

At1g51360rv	TGAAAGTCCCACAAACAACCA
GK T-DNA for At1g51360 insertion	TCAAACCCGGCAGCTTAGTT

Acknowledgements: We thank Andrew Fleming and Alice Baillie (University of Sheffield) for discussions at various stages of the project.

References

Abarca A, Franck CM, Zipfel C. 2021. Family-wide evaluation of RAPID ALKALINIZATION FACTOR peptides. Plant Physiology: kiab308. 1. DOI: 10.1093/plphys/kiab308

Alling R, Galindo Trigo S. 2023. Reproductive defects in the abscission mutant ida-2 are caused by T-DNA–induced genomic rearrangements. Plant Physiology. 193: 2292–2297. 2. DOI: 10.1093/plphys/kiad449

Alonso JM, Stepanova AN, Leisse TJ, Kim CJ, Chen H, Shinn P, et al., Ecker JR. 2003. Genome-wide insertional mutagenesis of Arabidopsis thaliana. Science. 301: 653–7. 11. PubMed ID: 12893945

Belling J, Blakeslee AF. 1926. On the attachment of non-homologous chromosomes at the reduction division in certain 25-chromosome Daturas. Proceedings of the National Academy of Sciences. 12: 7–11. 4. DOI: 10.1073/pnas.12.1.7

Camacho C, Coulouris G, Avagyan V, Ma N, Papadopoulos J, Bealer K, Madden TL. 2009. BLAST+: architecture and applications. BMC Bioinformatics. 10: 421. 19. PubMed ID: 20003500

Chen S, Zhou Y, Chen Y, Gu J. 2018. fastp: an ultra-fast all-in-one FASTQ preprocessor. Bioinformatics. 34: i884–i890. 14. PubMed ID: 30423086

Clark KA, Krysan PJ. 2010. Chromosomal translocations are a common phenomenon in Arabidopsis thaliana T-DNA insertion lines. The Plant Journal. 64: 990–1001. 6. DOI: 10.1111/j.1365-313X.2010.04386.x

Conrath U. 2024. Unlocking Precision in Callose Staining: Unveiling the Role of Sirofluor. Molecular Plant-Microbe Interactions®. 37: 595. 12. PubMed ID: 38739552

Curtis MJ, Belcram K, Bollmann SR, Tominey CM, Hoffman PD, Mercier R, Hays JB. 2009. Reciprocal chromosome translocation associated with TDNA-insertion mutation in Arabidopsis: genetic and cytological analyses of consequences for gametophyte development and for construction of doubly mutant lines. Planta. 229: 731–745. 5. DOI: 10.1007/s00425-008-0868-0

Galindo Trigo S, Blanco Tourinan N, De Falco TA, Wells ES, Gray JE, Zipfel C, Smith LM. 2020. CrRLK1L receptor-like kinases HERK1 and ANJEA are female determinants of pollen tube reception. EMBO Reports. 21: e48466. 13. PubMed ID: 31867824

Kleinboelting N, Huep G, Kloetgen A, Viehoever P, Weisshaar B. 2012. GABI-Kat SimpleSearch: new features of the Arabidopsis thaliana T-DNA mutant database. Nucleic Acids Res 40(Database issue): D1211-5. PubMed ID: 22080561

Lau YL. 2023. Functional analysis of Arabidopsis pollen coat proteins in the pollen-stigma interaction. 3.

Li H, Durbin R. 2010. Fast and accurate long-read alignment with Burrows-Wheeler transform. Bioinformatics. 26: 589–95. 15. PubMed ID: 20080505

Li H, Handsaker B, Wysoker A, Fennell T, Ruan J, Homer N, et al., Genome Project Data Processing S. 2009. The Sequence Alignment/Map format and SAMtools. Bioinformatics. 25: 2078–9. 16. PubMed ID: 19505943

Prjibelski A, Antipov D, Meleshko D, Lapidus A, Korobeynikov A. 2020. Using SPAdes De Novo Assembler. Curr Protoc Bioinformatics. 70: e102. 18. PubMed ID: 32559359

Pucker B, Kleinbolting N, Weisshaar B. 2021. Large scale genomic rearrangements in selected Arabidopsis thaliana T-DNA lines are caused by T-DNA insertion mutagenesis. BMC genomics. 22: 1–21. 7. DOI: 10.1186/s12864-021-07877-8

Raabe K, Sun L, Schindfessel C, Honys D, Geelen D. 2024. A word of caution: T-DNA-associated mutagenesis in plant reproduction research. Journal of Experimental Botany. 75: 3248–3258. 9. DOI: 10.1093/jxb/erae114

Robinson JT, Thorvaldsdottir H, Winckler W, Guttman M, Lander ES, Getz G, Mesirov JP. 2011. Integrative genomics viewer. Nat Biotechnol. 29: 24–6. 17. PubMed ID: 21221095

Thomson G, Dickinson L, Jacob Y. 2024. Genomic consequences associated with Agrobacterium-mediated transformation of plants. The Plant Journal. 117: 342–363. 8. DOI: https://doi.org/10.1111/tpj.16496

11/11/2026 - *Open Access*

Funding:
Supported by Biotechnology and Biological Sciences Research Council (United Kingdom) BB/W013754/1 to Lisa Smith.
Supported by Leverhulme Trust (United Kingdom) 2019-056 to Lisa Smith.

Conflicts of Interest: The authors declare that there are no conflicts of interest present.

Author Contributions: Jen Sloan: conceptualization, investigation, visualization, formal analysis, writing - original draft, writing - review editing. Yui-Leung Lau: conceptualization, investigation, writing - review editing. Amber Gentle: investigation, writing - review editing. Ellen Allwood: investigation. Volkan Cevik: investigation. James Doughty: conceptualization, supervision, writing - review editing. Lisa M Smith: data curation, supervision, funding acquisition, investigation, formal analysis, visualization, writing - original draft, writing - review editing.

Reviewed By: Anonymous

History: Received September 1, 2026 **Revision Received** October 23, 2026 **Accepted** November 2, 2026 **Published Online** November 11, 2026 **Indexed** November 25, 2026

Copyright: © 2026 by the authors. This is an open-access article distributed under the terms of the Creative Commons Attribution 4.0 International (CC BY 4.0) License, which permits unrestricted use, distribution, and reproduction in any medium, provided the original author and source are credited.

Citation: Sloan J, Lau YL, Gentle A, Allwood E, Cevik V, Doughty J, Smith LM. 2026. An Arabidopsis *RALF17 (AT2G32885)* GABI-Kat T-DNA line with two insertions has reproductive defects in the hemizygous state, possibly due to a genomic rearrangement. microPublication Biology. 10.17912/micropub.biology.002394